8th IFAC Symposium on Nonlinear Control Systems
University of Bologna, Italy, September 1-3, 2010

Stabilization of an Unmanned Bicycle with Flywheel Balancer

Lychek Keo * **Sirichai Pornsarayouth** * **Masaki Yamakita** *
Kazuhiro Ito **

* *Faculty of Mechanical and Control Engineering, Tokyo Institute of Technology, 2-12-1 Okayama, Meguro-ku, Tokyo, Japan 152-8552 (e-mail: {lychek,sirichai,yamakita}@ac.ctrl.titech.ac.jp)*
** *Science and Advanced Instruction & Control Equipments Co., 5-23-1 Higashigotanda, Shinagawa-Ku, Tokyo, Japan 141-0022 (e-mail: ito@saice.co.jp)*

Abstract: In this paper, a new balancer configuration for stabilization of an unmanned bicycle and a new switching control algorithm are proposed. The balancer can be configured as a flywheel or a balancer by shifting the center of gravity of the balancer. This balancer configuration changes according to the lean angle and/or the balancer angle, which causes change of the dimension of the system. The balancer is configured as a flywheel, when disturbances to the system are large and switches to a balancer when we have to shift the position of the center of gravity for reasons. Stabilizing bicycle with the flywheel has better performance than the balancer but this configuration cannot be controlled to shift the lean angle to track the desired value, unlike the balancer. The balancing controller is derived based on an output-zeroing controller. The parameters of the balancing control are switched based on the configuration of the balancer. Numerical simulation results are shown to verify the effectiveness of the proposed control strategy.

Keywords: Balancing Control; Output-Zeroing; Autonomous Bicycle; Balancer; Flywheel.

1. INTRODUCTION

Stabilization and trajectory tracking of unmanned bicycle is a popular topic for researchers in the latter half of the last century. Balancing a bicycle at low or zero linear velocity is a challenging control task. Literatures of bicycle stabilization are comprehensively reviewed from a control theory perspective in ([1],[2]), which also describes interesting bicycle-related experiments. Most of those papers focus on stabilizing a bicycle with the steering handlebar. From their simulation and experimental results, we can see that the region of stability is not so large. The bicycle model that is developed by Getz [3] cannot be controlled when the linear velocity is zero. Later, Yi [4] has modified this bicycle model by adding the bicycle caster angle. The modified model can use for stabilizing at the zero linear velocity. In order to enlarge the region of stability, the researchers have tried to use different mechanical designs to stabilize the bicycle at zero speed. In [5], unmanned bicycle robot with a flywheel namely Murata Boy was constructed and realized. It can be stabilized whether the bicycle runs or stops. In our Lab, we successfully use a balancer to stabilize the bicycle with zero or nonzero linear velocity ([6], [7], [8]), but the results does not satisfy our goal. Thus, we try to enlarge the region of stability by using both balancer and steering ([9], [10]), and it is shown that the input amplitude is suppressed very well. Also, Hwang [11] successfully use a steering handlebar and a balancer to stabilize the bicycle at zero speed but it cannot track a given trajectory. The aim of this paper is to propose a new balancer mechanical design and the switching law. Though the proposed mechanism can be easily incorporated with steering control, we focused on the stabilization when the bicycle stops and did not add a steering and a rear wheel into the model.

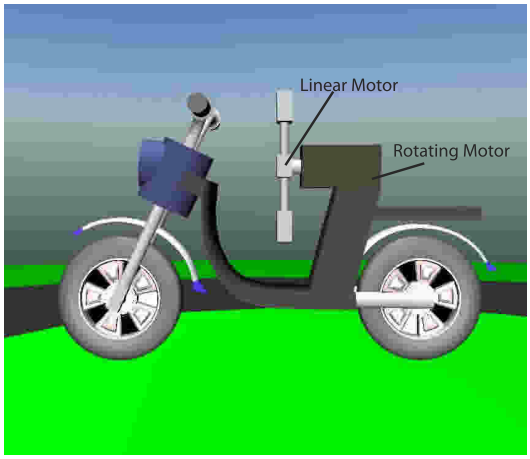

Fig. 1. Simulated bicycle with flywheel balancer.

Fig. 1 shows a new balancer configuration which is attached to a bicycle. This new balancer have two motors, one is a rotating motor which is used for rotation of the balancer. The another motor is a linear motor which is used for shifting the center of gravity of the balancer. With these configurations, we can use the balancer as a flywheel mode (Fig. 2a) or a balancer mode (Fig. 2b). The

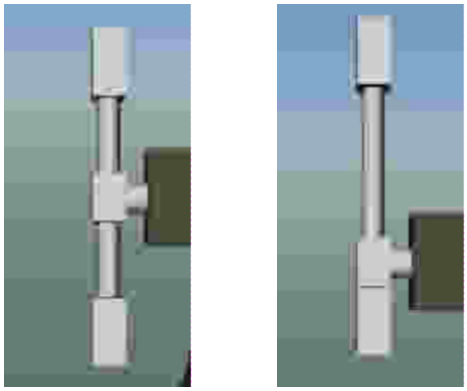

(a) Flywheel mode (b) Balancer mode

Fig. 2. Flywheel balancer configurations.

balancer is configured as a flywheel, when disturbances to the system are large, and switch to the balancer mode when we have to shift the center of gravity. An advantage of the flywheel is that we can stabilize the bicycle with large region of stability. On the other hand, advantages of the balancer is an ability to avoid the bicycle body from obstacles. The simplified dynamic model of this system was developed in [12]. The balancing controller is derived based on output-zeroing controller. The parameters of the balancing control are switched based on the configuration of the balancer. The proposed method can improve the performance and enlarge the region of stability of the bicycle. This paper is composed of five sections. In section II, we present a simplified dynamic model of the bicycle with a balancer. In section III, we discuss a control system design for stabilizing the bicycle. Numerical simulation results are presented in section IV. The conclusions are summarized in section V.

2. BICYCLE WITH BALANCER DYNAMICS

In this section, we present a bicycle with a flywheel balancer model based on an inverted pendulum model. A detailed model of a bicycle is complex since the system has many degrees of freedom. The coordinate system used for analyzing the bicycle is defined in Fig. 3. We consider the bicycle as a point mass with two wheels contact with the ground, and we consider the bicycle and the balancer as a two link system where the first link is the bicycle body with steering and the second link is the balancer. We assume that the bicycle moves on a horizontal plane and that the wheels always maintain contact with the ground. The wheels of the bicycle are considered to have negligible inertial moments, mass, thicknesses and no slip angle for both front and rear wheels. We will define α as the roll angle and β as the balancer angle. The bicycle and the balancer parameters are shown in Table I. The height of the balancer to the center of gravity (h_b) varies from $0m$ to $0.3m$ and the balancer becomes flywheel when h_b is zero. From [12], we can obtain the bicycle with flywheel

Table 1. The bicycle with balancer parameters

Parameter descriptions	Par.	Value
Bicycle mass	m	35 kg
Height of the bicycle center of mass	h	0.3 m
Moment inertia of bicycle at COG	I	0.35 kgm^2
Distance between ground and balancer	l	0.68 m
Balancer mass	m_b	9.5 kg
Moment inertia of balancer at COG	I_b	0.08 kgm^2

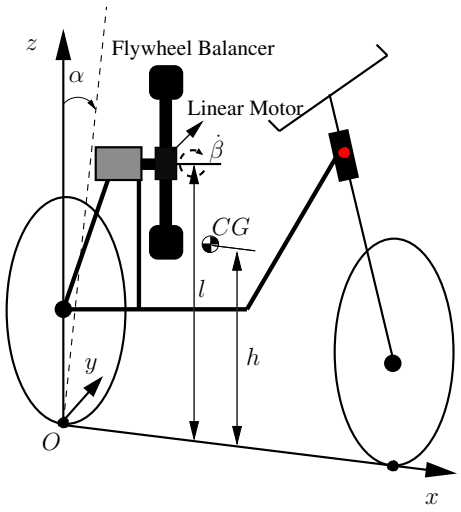

Fig. 3. Coordinate system of the bicycle with the balancer.

dynamics model as

$$\begin{bmatrix} M_{11} & M_{12} \\ M_{21} & M_{22} \end{bmatrix} \begin{bmatrix} \ddot{\alpha} \\ \ddot{\beta} \end{bmatrix} = \begin{bmatrix} K_1 \\ K_2 \end{bmatrix} + \begin{bmatrix} 0 \\ 1 \end{bmatrix} \tau_b \qquad (1)$$

,

where τ_b is the balancer torque input and

$$\begin{aligned} M_{11} &= I + I_b + mh^2 + m_b(h_b^2 + l^2 + 2h_b l\cos(\beta)), \\ M_{12} &= M_{21} = I_b + h_b m_b(h_b + l\cos\beta), \\ M_{22} &= I_b + h_b^2 m_b, \\ K_1 &= hmg\sin\alpha + m_b(g(l\sin\alpha + h_b\sin(\alpha+\beta)) \\ &\quad + h_b l\dot{\beta}(2\dot{\alpha}+\dot{\beta})\sin\beta), \\ K_2 &= h_b m_b(-l\dot{\alpha}^2\sin\beta + g\sin(\alpha+\beta)). \end{aligned}$$

This gives us a simplified model that we can use for designing the controllers for the bicycle stabilization.

3. CONTROL ALGORITHM

In order to improve the stabilizing performance, we introduce a new balancer configuration as described in section I. We use the flywheel to stabilize the bicycle when the system is starting up or the disturbances to the system are large. Flywheel cannot control to shift the bicycle body for long time, thus the balancer becomes useful when we want to shift the bicycle angle to desired value. We use output-zeroing controller to stabilize the bicycle using flywheel or balancer mode. The basic idea of output-zeroing controller is that an output function is defined so that the relative degree from the input to the output becomes three and the zero dynamic becomes stable. Then, the output-zeroing controller is designed. In this case, a new state is defined so that the new output function is easily determined since the angular momentum is integrable for two D.O.F. system. When the balancer system changes the configuration, the control parameters also change accordingly. Thus, we introduce the switching controller to switch the parameters of the balancing controller.

3.1 Model of two-link system

By projecting the motion of the balancer on YZ plane, the system can be considered as a two-link system (Fig. 4).

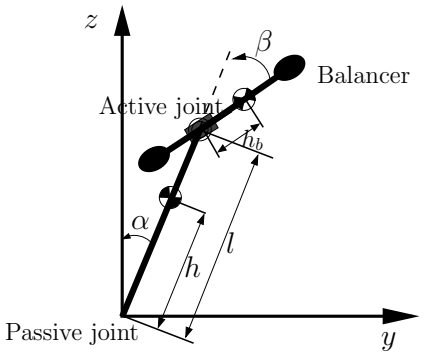

Fig. 4. Two-Link System.

In the two-link model, the bicycle body and steering handlebar consist of the first link, the balancer with the linear motor is considered as the second link. The control torque for the system is applied to the second joint of the balancer. We can find the angular momentum L from the first row of (1) as

$$\begin{aligned} L &= M_{11}\dot{\alpha} + M_{12}\dot{\beta} \\ &= (d_1 + d_3 + 2d_2\cos\beta)\,\dot{\alpha} + (d_3 + d_2\cos\beta)\,\dot{\beta}, \end{aligned} \tag{2}$$

where $d_1 = I + mh^2 + m_b l^2$, $d_2 = m_b l h_b$, $d_3 = m_b h_b^2 + I_b$, and it can be easily shown that the time derivative of L just contains a gravity term of K_1 and it is calculated as

$$\dot{L} = e_1 \sin\alpha + e_2 \sin(\alpha + \beta), \tag{3}$$

where $e_1 = g(mh + m_b l)$ and $e_2 = g m_b h_b$. Using the angular momentum expressed in (2), a new function p is defined to satisfy the following:

$$L = (d_1 + d_3 + 2d_2\cos\beta)\,\dot{p}. \tag{4}$$

From the equation above, p can be determined as

$$p = \alpha + \int_{\beta_0}^{\beta} \frac{d_3 + d_2\cos\beta}{d_1 + d_3 + 2d_2\cos\beta} d\beta - C = \alpha + w(\beta), \tag{5}$$

where C is an integral constant and is determined as $p = 0$ when the system is at the upright position. Using L and p, a new coordinate function $q = (p, L, \beta, \dot{\beta})$ can be represented as

$$\begin{bmatrix} \dot{p} \\ \dot{L} \\ \dot{\beta} \\ \ddot{\beta} \end{bmatrix} = \begin{bmatrix} L/H(\beta) \\ G(p,\beta) \\ \dot{\beta} \\ 0 \end{bmatrix} + \begin{bmatrix} 0 \\ 0 \\ 0 \\ 1 \end{bmatrix} u_b, \tag{6}$$

where $H(\beta) := d_1 + d_3 + 2d_2\cos\beta$,, $G(p,\beta) := e_1\sin(p - w(\beta)) + e_2\sin(p - w(\beta) + \beta)$, and u_b a new input defined as $u_b := \ddot{\beta}$.

3.2 Output-zeroing controller

For the system (6), an output function y is defined as

$$y = L + a_1 p, \tag{7}$$

where $a_1 = 0$ if the balancer is configured as flywheel and $a_1 > 0$ if the height of the balancer $h_b > 0$ and it is controlled to zero since

$$y = 0 \quad \rightarrow \dot{p} = (-a_1/H)p \;\text{ and }\; \dot{L} = -a_1\dot{p},$$

this zero dynamics is stable. Since L and p have three relative degrees to the control input, we can easily determine a control input which attains the dynamics of the output function. By taking third derivative of y, we have

$$y^{(3)} = L^{(3)} + a_1 p^{(3)}, \tag{8}$$

$$\ddot{L} = \frac{dG}{dt} = \frac{\partial G}{\partial p}\frac{L}{H} + \frac{\partial G}{\partial \beta}\dot{\beta}, \tag{9}$$

$$L^{(3)} = \frac{d}{dt}\left(\frac{\partial G}{\partial p}\frac{L}{H}\right) + \frac{d}{dt}\left(\frac{\partial G}{\partial \beta}\right)\dot{\beta} + \frac{\partial G}{\partial \beta}u_b, \tag{10}$$

$$\ddot{p} = \frac{G}{H} - \frac{(\partial H/\partial\beta)\,L}{H^2}\dot{\beta}, \tag{11}$$

$$\begin{aligned} p^{(3)} = {} & \frac{d}{dt}\left(\frac{G}{H}\right) - \frac{d}{dt}\left(\frac{(\partial H/\partial\beta)\,L}{H^2}\right)\dot{\beta} \\ & - \frac{(\partial H/\partial\beta)\,L}{H^2}u_b. \end{aligned} \tag{12}$$

We can determine a control input which attains the dynamics of the output function as

$$y^{(3)} + a_2\ddot{y} + a_3\dot{y} + a_4 y = 0, \tag{13}$$

and y converges to zero asymptotically if $a_2 > 0$, $a_3 > 0$, $a_4 > 0$ are design parameters and they are determined so that the following system is Hurwitz (other robust stabilizing controls of y can be also used).
By rearranging the equations from (8) to (13) and we can put it in the form of

$$\begin{aligned} u_b = {} & \left(\frac{\partial G}{\partial \beta} - a_1\frac{(\partial H/\partial\beta)\,L}{H^2}\right)^{-1}\left(-\frac{d}{dt}\left(\frac{\partial G}{\partial p}\frac{L}{H}\right)\right. \\ & -\frac{d}{dt}\left(\frac{\partial G}{\partial \beta}\right)\dot{\beta} - a_1\frac{d}{dt}\left(\frac{G}{H}\right) \\ & \left. +a_1\frac{d}{dt}\left(\frac{(\partial H/\partial\beta)\,L}{H^2}\right)\dot{\beta} - a_2\ddot{y} - a_3\dot{y} - a_4 y\right). \end{aligned} \tag{14}$$

The parameters a_1, a_2, a_3 and a_4 are varied depending on the balancer configuration change.

3.3 Switching law

The control objective is to stabilize the bicycle at the upward unstable equilibrium position. As introduced in Section I, there have two configurations for the balancer. The configuration is changed according to the lean angle and the balancer angle. The balancer is configured as a flywheel mode, when the disturbances to the system are large or when the system is starting up and it will switch to the balancer mode when the system is in the stabilizable region with it. One of the switching law is shown in Fig. 5 and we can switch the balancing control parameters as

$$\begin{aligned} & \{a_1, a_2, a_3, a_4\} = \\ & \begin{cases} \{a_1^1, a_2^1, a_3^1, a_4^1\}, \text{ if } |\alpha| \le |\alpha_1| \& |\beta| \le |\beta_1|; \\ \{a_1^2, a_2^2, a_3^2, a_4^2\}, \text{ else.} \end{cases} \end{aligned} \tag{15}$$

The maximum bicycle angle is limited to α_2 and β_1 is the switching angle of the balancer. The parameters with index

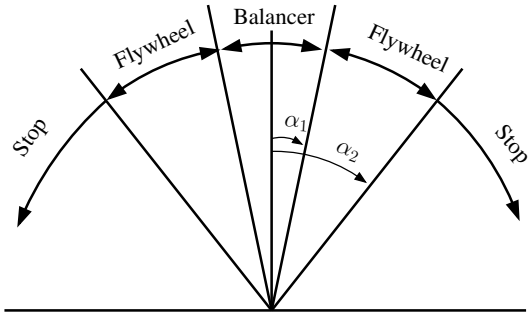

Fig. 5. Switching between flywheel and balancer.

1 are the control parameters for the balancer mode and the parameters with index 2 are the control parameters for the flywheel mode. It is noted that the parameter a_1^2 is usually set to zero; Because in the flywheel mode, we don't care much about the balancer angle though the angular velocity is controlled to zero. Please note that the dimension of the system state is changed due to the change of the configuration while the controller structure remains fixed.

4. NUMERICAL SIMULATION

The simulation is conducted on an Intel Core 2 Duo, 2.2GHz, 2GB RAM computer, and all simulations were performed in MATLAB using an adaptive step-size Runge-Kutta integrator, ode45. In order to explain the effectiveness of the proposed method, several numerical simulations are shown where the parameters of the bicycle are shown in Table I. The limitation of the control input for the balancer is set to 100[Nm]. To show the validity of the proposed control for the bicycle stabilization, we perform three types of simulation to compare the response of the bicycle stability.

4.1 Stabilizing the bicycle with a balancer

In this simulation, the balancer is used to stabilize the bicycle and the height of the center gravity of the balancer is set to $0.3m$. The control parameters are set to $a_1 = 40$, $a_2 = 22$, $a_3 = 35$ and $a_4 = 15$. The initial angles of the bicycle and balancer are set to $\alpha_0 = 10°$ and $\beta_0 = -10°$. Fig.6a shows the angles of α, β versus time which converge to the upright position. The angular velocity of the bicycle and the balancer are shown in Fig.6b. The maximum torque for the balancer is 75.5[Nm] and it is shown in Fig.6c. From Fig.6d, it is shown that the zero dynamic output function converges to zero. The balancer can stabilize the bicycle within the roll angle 10°. If there are disturbances that make the bicycle angle larger than 10°, thus the bicycle cannot control by the balancer. The good point of the balancer is that we can control the bicycle angle to track the desired value. Fig.7 shows that the bicycle angle tracks the desired value. In this figure, the solid line represents the bicycle angle, the dotted line is the desired bicycle angle and the dashed line is the balancer angle.

4.2 Stabilizing the bicycle with a flywheel

In this simulation, the balancer is configured as the flywheel. Thus, the balancer is rotated around the center

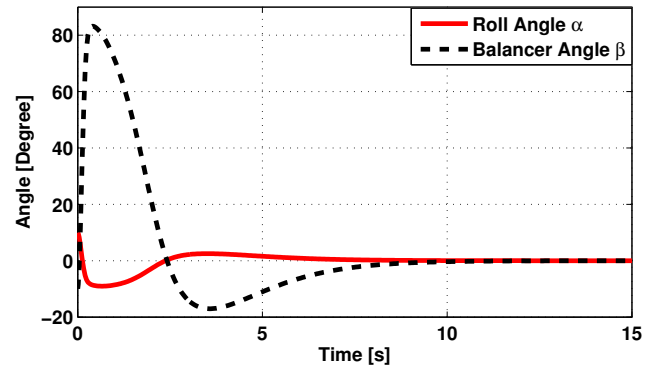

(a) Roll angle α, Balancer angle β

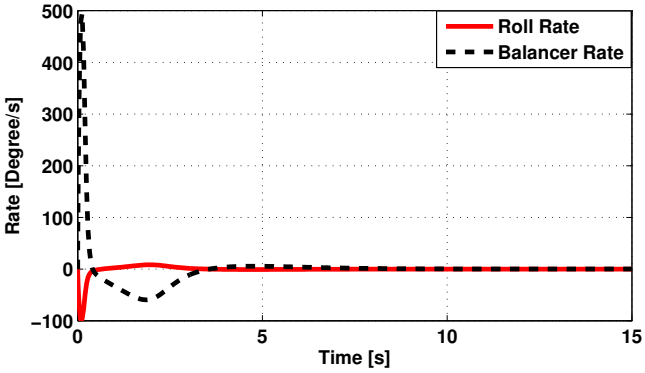

(b) Roll angular velocity $\dot{\alpha}$, Balancer angular velocity $\dot{\beta}$

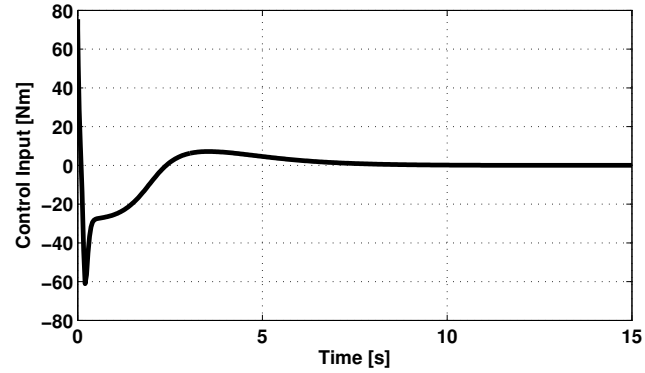

(c) Balancer torque τ_b

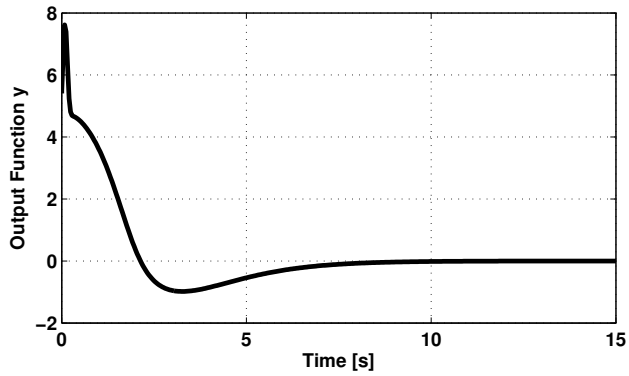

(d) Output Function y

Fig. 6. Bicycle stabilization with the balancer

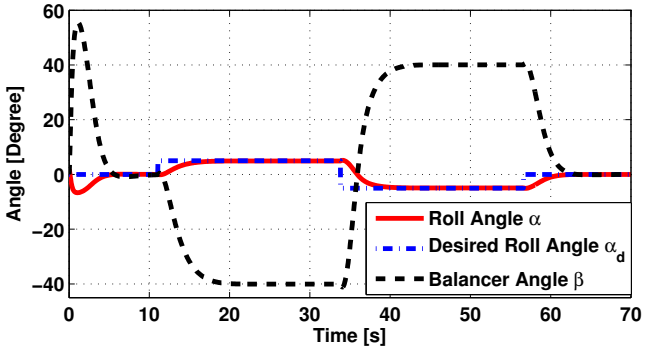

Fig. 7. Tracking desired bicycle angle

of gravity and the height of the balancer to the center of gravity is zero ($h_b = 0$). The control parameters are set to $a_1 = 0$, $a_2 = 3$, $a_3 = 10$, and $a_4 = 10$. The initial angle of the bicycle is set to $\alpha_0 = 10°$. Fig.8a shows the bicycle angle α and angular velocity $\dot{\alpha}$ versus time. It is shown that the bicycle angle converges to the upright position within $5s$. Fig.8b shows the flywheel angle β and angular velocity $\dot{\beta}$ versus time. From this figure, we can see that the flywheel angle does not converge to zero, but the flywheel angular velocity converges to zero. The maximum torque for the flywheel is 42[Nm] that is shown in Fig.8c and it is required less torque than balancing the bicycle with the balancer. Fig. 8d shows that the output function y converges to zero. When the flywheel angle does not converge to zero, we cannot switch the control parameters to control the balancer. Thus, we modified the control parameters as $a_1 = 4$, $a_2 = 3$, $a_3 = 10$, $a_4 = 10$ and the parameter a_1 cannot be large. Since the parameter a_1 is not zero, the flywheel angle will slowly converge to zero. The result is shown in Fig.9.

4.3 Stabilizing the bicycle with flywheel balancer

Since the flywheel and the balancer have different advantages for stabilizing the bicycle, we used both to stabilize the bicycle. The flywheel mode is used when the disturbances to the system are large or the system is starting up and it will switch to the balancer mode when the system is in the stabilizable region with it. In the system startup mode, the control parameters are set to $a_1 = 1.5$, $a_2 = 3$, $a_3 = 8$, $a_4 = 8$ and these control parameters will switch to $a_1 = 40$, $a_2 = 22$, $a_3 = 35$, and $a_4 = 15$ when the bicycle and balancer angle met the condition as $|\alpha| \leq 10°$ and $|\beta| \leq 10°$. To show the robustness of the balancing controller, we add noises into the output state $(\alpha, \beta, \dot{\alpha}, \dot{\beta})$. The results is shown in Fig.10. When the switching law met the condition at time $t = 6s$, the balancer switch the mode from the flywheel to the balancer with in $1.5s$. From this figure, we can see that the new balancer configuration works very well.

5. CONCLUSIONS

In this paper, a new balancer configuration and switching control law for stabilizing an unmanned bicycle are proposed. The balancing control and switching law are fully discussed. From the simulation results, the stabilized bicycle with flywheel has better performance than balancer

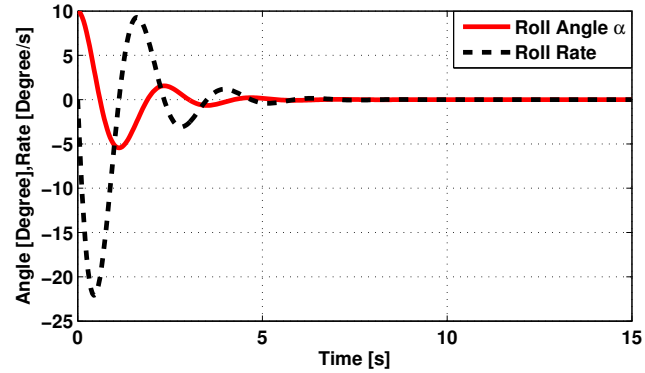

(a) Roll angle α

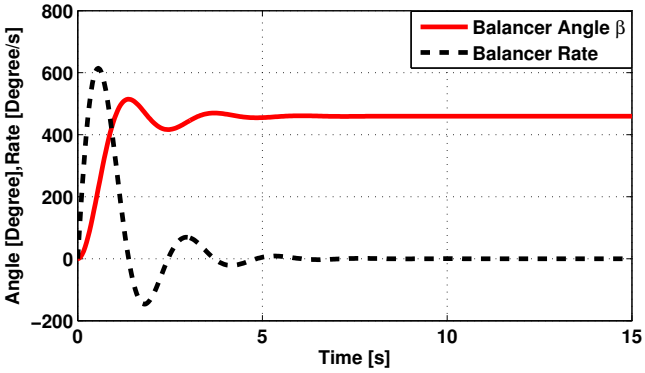

(b) Balancer angle β, Balancer angular velocity $\dot{\beta}$

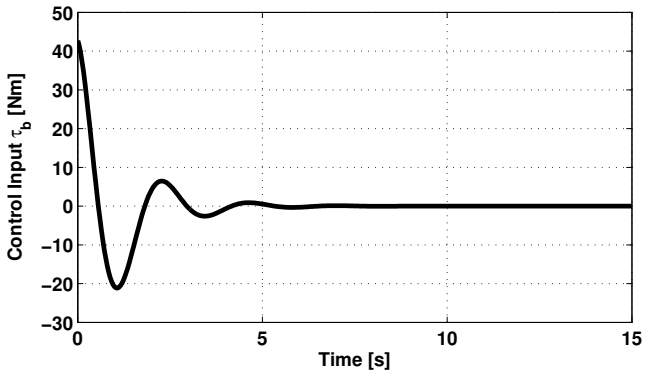

(c) Balancer torque τ_b

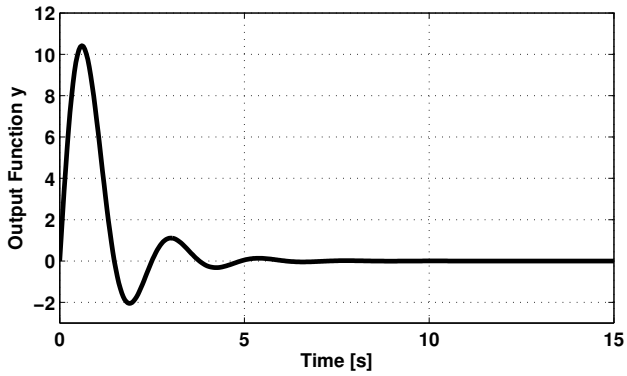

(d) Output Function y τ_b

Fig. 8. Bicycle stabilization with the flywheel and $a_1 = 0$

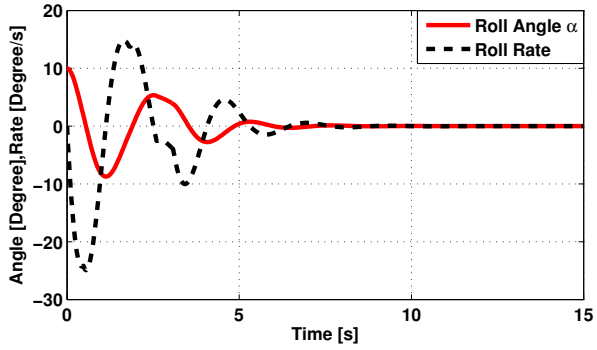

(a) Roll angle α

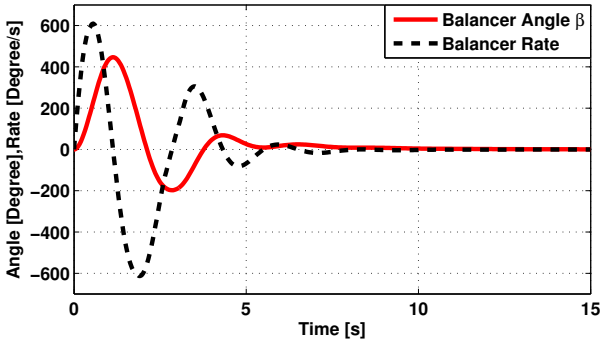

(b) Balancer angle β, Balancer angular velocity $\dot{\beta}$

Fig. 9. Bicycle stabilization with the flywheel and a_1 is small

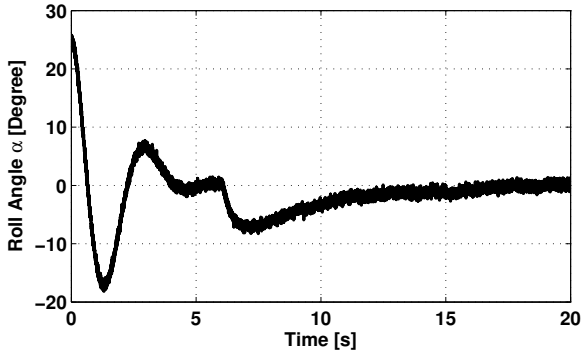

(a) Roll angle α

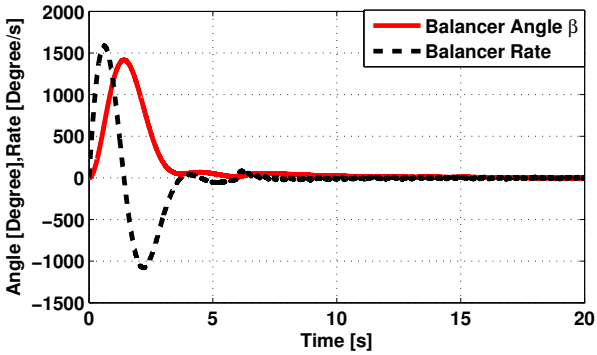

(b) Balancer angle β, Balancer angular velocity $\dot{\beta}$

Fig. 10. Bicycle stabilization with the flywheel balancer

but it cannot control to shift the bicycle angle to track the desired value, unlike the balancer which can perform this task. Since the flywheel and the balancer have different advantages, we used both to stabilize the bicycle. The flywheel is used when the disturbances to the system are large or at startup mode and it will switch to the balancer when the system is in the stabilizable region with it. Experimental validation of this system is currently in progress. In the future, we intend to use this system for stabilizing the bicycle with trajectory tracking at high speed.

REFERENCES

[1] K. Astrom, R. Klein and A.Lennartsson , "Bicycle Dynamics and Control," *IEEE Control System Magazine*, vol. 25, no. 4, pp. 26-47, 2005.

[2] R.S. Sharp,"The Stability and Control of Motorcycles," *Journal Mechanical Engineering Science*, vol.13, no. 5, pp.316-329, 1971.

[3] N. Getz, "Dynamic Inversion of Nonlinear Maps with Applications to Nonlinear Control and Robotics," *Ph.D dissertation, Department of Electrical Engineering and Computer Sciences*, University of California at Berkeley, CA, 1995.

[4] J. Yi, D. Song, A. Levandowski and S. Jayasuriya, "Trajectory Tracking and Balance Stabilization Control of Autonomous Motorcycle," *Proceeding IEEE Int. conf. on Robotics and Automation*, pp. 2583-2589, 2006.

[5] Murata Manufacturing Co. Ltd "Murata boy" *website* http://www.murataboy.com , 2006.

[6] M. Yamakita and A. Utano, "Automatic Control of Bicycle with Balancer," *IEEE/ASME Int. Conf. on Advanced Intelligent Mechatronics*, pp. 1245-1249, 2005.

[7] M. Yamakita, A. Utano and K. Sekiguchi, "Experimental Study of Automatic Control of Bicycle with Balancer," *IEEE/ASME Int. Conf. on Advanced Intelligent Mechatronics*, pp. 1245-1249, 2005.

[8] L. Keo and M. Yamakita, "Trajectory Control for an Autonomous Bicycle with Balancer," *IEEE/ASME Int. Conf. on Advanced Intelligent Mechatronics*, pp. 676-681, 2008.

[9] L. Keo and M. Yamakita, "Controller Design of an Autonomous Bicycle with Both Steering and Balancer Controls," *IEEE/MSC IEEE Int. Conf. on Control Applications*, pp. 1294-1299, 2009.

[10] L. Keo and M. Yamakita, "Controlling Balancer and Steering for Bicycle Stabilization," *IEEE/RSJ Int. Conf. on Intelligent Robots and Systems*, pp. 4541-4546, 2009.

[11] C. Hwang, H. Wu and C. Shih, "Autonomous Dynamic Balance of an Electrical Bicycle Using Variable Structure Under-Actuated Control," *IEEE/RSJ International Conference on Intelligent Robots and Systems*, pp. 3737-3743, 2008.

[12] L. Keo and M. Yamakita, "Dynamic Models of a Bicycle with a Balancer System," *The 26th annual conference of the Robotics Society of Japan*, pp. 43-46, 2008.